Zebrafish embryo screen identifies anti-metastasis drugs

Joji Nakayama[1,2,3,4§], Lora Tan[1], Boon Cher Goh[2], Shu Wang[1, 5], Hideki Makinoshima[3,6] and Zhiyuan Gong[1§]

[1]Department of Biological Science, National University of Singapore, Singapore
[2]Cancer Science Institute of Singapore, National University of Singapore, Singapore
[3]Tsuruoka Metabolomics Laboratory, National Cancer Center, Tsuruoka, Japan
[4]Shonai Regional Industry Promotion Center, Tsuruoka, Japan.
[5]Institute of Bioengineering and Nanotechnology, Singapore
[6]Division of Translational Research, Exploratory Oncology Research and Clinical Trial Center, National Cancer Center, Kashiwa, Japan.

Keywords: Zebrafish, metastasis, gastrulation, phenotyping screening

[§]Corresponding authors:
Joji Nakayama
Tsuruoka Metabolomics Laboratory, National Cancer Center, Mizukami 246-2, Kakuganji, Tsuruoka, Yamagata, Japan 975-0052.
email: Zmetastasis@gmail.com

Zhiyuan Gong
Department of Biological Science, National University of Singapore, Singapore 117543.
email: dbsgzy@nus.edu.sg

The authors disclose no potential conflicts of interest.

Total words excluding abstract, material and methods, references, and figure legends: 1390

Number of figures: 2
Number of supplementary figures: 3
Number of supplementary tables: 3

Abstract

Metastasis is responsible for approximately 90% of cancer-associated mortality, but few models exist that allow for rapid and effective screening of anti-metastasis drugs. Here we report a novel screening concept utilizing conserved mechanisms between metastasis and zebrafish gastrulation for identifying anti-metastasis drugs. Molecular mechanisms involved in metastasis and vertebrate gastrulation are conserved; at least fifty common genes play essential roles in governing these mechanisms. We hypothesized that small chemicals that interrupt zebrafish gastrulation might also suppress metastatic progression of cancer cells and developed a phenotype-based chemical screen to test the hypothesis. The screen used epiboly, the first morphogenetic movement in gastrulation as a marker, and identified a serotonin receptor 2C (HTR2C) antagonist as an epiboly-interrupting drug. A mouse model of metastasis confirmed that pharmacologic and genetic inhibition of HTR2C suppressed metastasis. Taken together, this screen could offer a rapid and high-throughput platform for discovery of anti-metastasis drugs.

46 **Introduction**

47 Metastasis, a leading contributor to the morbidity of cancer patients, occurs through multiple
48 steps: invasion, intravasation, extravasation, colonization, and metastatic tumor formation.
49 The physical translocation of cancer cells is an initial step of metastasis and molecular
50 mechanisms of it involve cell motility, the breakdown of local basement membrane, loss of
51 cell polarity, acquisition of stem cell-like properties, and epithelial-mesenchymal transition
52 (EMT) (1, 2). These cell-biological phenomena are also observed during vertebrate
53 gastrulation in that evolutionarily conserved morphogenetic movements of epiboly,
54 internalization, convergence, and extension progress (3). In zebrafish, the first morphogenetic
55 movement, epiboly, is initiated at approximately 4 hours post fertilization (hpf) to move cells
56 from the animal pole to eventually engulf the entire yolk cell by 10 hpf (4, 5). The embryonic
57 cell movements are governed by the molecular mechanisms that are partially shared in metastatic
58 cell dissemination.

59 At least fifty common genes play essential roles in both metastasis and gastrulation
60 (Supplementary Table 1): Knockdown of these genes in zebrafish induced gastrulation
61 defects; conversely, overexpression of these genes conferred metastatic potential on cancer
62 cells while knockdown of these genes suppressed metastasis. Based on this evidence, we
63 hypothesized that small chemicals that interrupt zebrafish gastrulation might also suppress
64 metastatic progression of cancer cells.

65 Here we report a novel screening concept utilizing conserved mechanisms between
66 metastasis and zebrafish gastrulation for identifying anti-metastasis drugs. The screen which
67 used epiboly, the first morphogenetic movement in gastrulation as a marker, identified a
68 serotonin receptor 2C (HTR2C) antagonist as an epiboly-interrupting drug, and a mouse
69 model of metastasis confirmed pharmacologic and genetic inhibition of HTR2C suppressed
70 metastasis.

71

72 **Results**

73 We first conducted experiments of whether hindering the molecular function of protein
74 arginine methyltransferase 1 (PRMT1) and cytochrome P450 family 11 (CYP11A1), whose
75 knockdown induced gastrulation defects in zebrafish but whose involvement in metastasis is
76 unclear might suppress cell motility and invasion of cancer cells (6)(7). Knockdown of
77 PRMT1 or CYP11A1 suppressed the motility and invasion of metastatic human cancer cells
78 (Supplementary Figure 1A-C). Furthermore, we conducted an inverse examination of whether
79 Niclosamide and Vinpocetine which suppress metastatic dissemination of cancer cells, could
80 interrupt epiboly of zebrafish embryos (8)(9). Zebrafish embryos treated with either
81 Niclosamide or Vinpocetine showed complete arrest or severe delay in epiboly, respectively
82 (Supplementary Figure 1D). Thus, epiboly could serve as a marker for a screening assay and
83 epiboly-interrupting drugs could potentially suppress metastasis of human cancer cells.

84 We screened 1,280 FDA, EMA or other agencies-approved drugs (Prestwick, Inc) in
85 zebrafish epiboly inhibition assay. The screening showed that 0.9% (12/1280) of the drugs,
86 including Actimycin A and Tolcapone, induced severe or complete arrest of embryonic cell
87 movement when embryos were treated with 10μM concentration. 5.2% (66/1280) of the
88 drugs, such as Dicumarol, Racecadotril, Pizotifen and S(-) Eticlopride hydrochloride, induced
89 either delayed epiboly or interrupted epiboly of the embryos. 93.3% (1194/1280) of the drugs
90 had no effect on epiboly. 0.6% (8/1280) of the drugs induced toxic lethality. Epiboly
91 progression was affected more severely when embryos were treated with 50 μM
92 concentration (Figure 1A, Supplementary Figure 1E and Supplementary Table 2). Among the
93 epiboly-interrupting drugs, Adrenosterone, Zardaverine, Racecadotril and Disulfiram have
94 already been reported to inhibit metastasis-related molecular mechanisms (10-13). This
95 evidence supports that epiboly-interrupting drugs have the potential to suppress metastasis of
96 human cancer cells.

97 We subjected the 78 epiboly-interrupting drugs that showed a suppressor effect on
98 epiboly progression at a 10μM concentration to *in vitro* examination of whether the drugs
99 could suppress cell motility and invasion of MDA-MB-231 cells through a Boyden chamber
100 assay. Sixteen of the 78 drugs strongly affected cell viability and were excluded. The
101 remaining 62 drugs were subjected to the assay, and twenty of the 62 drugs inhibited cell
102 motility and invasion of the cells without affecting cell viability (Figure 1B). Among the 20
103 drugs, three drugs: Hexachlorophene, Nitazoxanide and Ipriflavone were removed since the
104 primary targets of the drugs, are either not expressed in mammalian cells or unknown. The
105 known primary targets of the remaining 17 drugs are reported to be expressed by mammalian
106 cells (Supplementary Table 3). Among the 17 drugs, Pizotifen and S(-) Eticlopride
107 hydrochloride suppressed cell motility and invasion of several highly metastatic human
108 cancer cell lines in a dose-dependent manner (Figure 1C and supplementary Figure 2A).
109 We selected Pizotifen as a candidate drug for blocking metastasis since its primary
110 target, serotonin receptor 2C (HTR2C), was highly expressed only in metastatic cell lines
111 (Figure 1D). Furthermore, HTR2C induced EMT on human epithelial cells and promoted
112 metastatic dissemination of human cancer cells in a zebrafish xenotransplantation model
113 (Supplementary Figure 3A-E); conversely, pharmacologic and genetic inhibition of HTR2C
114 suppressed metastatic dissemination of highly metastatic human cancer cells in the model
115 (Figure 1E and supplementary Figure 2B&C).
116 Finally, we validated the metastasis-suppressor effect of Pizotifen in a mouse model
117 of metastasis(14). Luciferase-expressing 4T1 murine mammary carcinoma cells were
118 inoculated into the mammary fat pads (MFP) of female BALB/c mice. Bioluminescence
119 imaging and tumor measurement revealed no anti-tumor effect of Pizotifen on the primary
120 tumor (Figure 2A&B). After 70 days from the inoculation, bioluminescence imaging detected
121 light emitted in the lungs, livers and lymph nodes of vehicle-treated mice but not those of

122 Pizotifen-treated mice (Figure 2B). Vehicle-treated mice formed 5 to 50 metastatic nodules
123 per lung in all 10 mice analyzed; conversely, Pizotifen-treated mice (n=10) formed 0 to 5
124 nodules per lung in all 10 mice analyzed (Figure 2C). Histological analyses confirmed that
125 metastatic lesions in the lungs in all vehicle-treated mice; conversely, they were detected in
126 only 2 Pizotifen-treated mice and the rest 8 mice showed metastatic colony formations
127 around the bronchiole of the lung. In addition, 4 of 10 vehicle-treated mice exhibited
128 metastasis in the liver and the rest showed metastatic colony formation around the portal tract
129 of the liver. In contrast, none of 10 Pizotifen-treated mice showed liver metastases and only 5
130 mice showed metastatic colony formation around the portal tract (Figure 2D). These results
131 indicate that Pizotifen can suppress metastasis progression without affecting primary tumor
132 growth.
133 To eliminate potential off-target effects of Pizotifen, we confirmed whether
134 knockdown of HTR2C would show the same effects. Sub-clones of 4T1 cells that expressed
135 shRNA targeting either LacZ (shLacZ_4T1) or HTR2C (shHTR2C_4T1) were injected into
136 the MFP of female BALB/c mice. All of the mice (n=5) that were inoculated with
137 shLacZ_4T1 cells showed metastases in the lungs; conversely, only one of the mice (n=5)
138 that were inoculated with shHTR2C_4T1 cells showed metastases in the lungs and the rest of
139 the mice did not. The mean number of metastatic lesions in the lung significantly decreased
140 to 10% of those of mice that were inoculated with shLacZ_4T1 cells (Figure 2E&F). These
141 results indicate that pharmacological and genetic inhibition of HTR2C showed an anti-
142 metastatic effect in the 4T1 model system.
143
144 **Discussion**
145 Reducing or eliminating mortality associated with metastatic disease is a key goal of medical
146 oncology, but few models exist that allow for rapid and effective screening of novel compounds

147 that target metastasis. We developed a unique screening concept utilizing zebrafish gastrulation
148 to identify anti-metastatic drugs. Our results clearly confirmed our hypothesis: 25.6% (20/76
149 drugs) of epiboly-interrupting drugs could also suppress cell motility and invasion of highly
150 metastatic human cell lines in vitro (Figure 1B). A mouse model of metastasis confirmed that
151 Pizotifen, which is one of the epiboly-interrupting drugs, could suppress metastasis (Figure
152 2A-C). Thus, this screen could offer a rapid and high-throughput platform for discovery of
153 anti-metastasis drugs.

154 There are at least two advantages to the screen described herein. One is that the screen
155 can easily be converted to a chemical genetic screening platform. Indeed, we have provided
156 the first evidence that HTR2C, which is a primary target of Pizotifen, induced EMT and
157 promoted metastatic dissemination of cancer cells (Supplementary Figure 3A-E). In this
158 research, 1,280 FDA approval drugs were screened, this is less than a few percent of all of
159 druggable targets (approximately 100 targets) in the human proteome in the body. If chemical
160 genetic screening using specific inhibitor libraries were conducted, more genes that contribute
161 to metastasis and gastrulation could be identified. The second advantage is that the screen
162 enables one researcher to test 100 drugs in 5 hours with using optical microscopy, drugs, and
163 zebrafish embryos. That indicates this screen is not only highly efficient, low-cost, and low-
164 labor but also enables researchers who do not have high throughput screening instruments to
165 conduct drug screening for anti-metastasis drugs.

166

167 **Materials and Methods**

168 Zebrafish embryo screening

169 Each drug was added to a well of a 24-well plate containing approximately 20 zebrafish
170 embryos per well in either 10 μM or 50 μM final concentration when the embryos reached
171 the sphere stage. Chemical treatment was initiated at 4 hours post-fertilization (hpf) and

172 approximately 20 embryos were treated with two different concentrations for each compound
173 tested. The treatment was ended at 9 hpf when vehicle (DMSO) treated embryos as control
174 reach 80-90% completion of the epiboly stage. The compounds which induced delay (<50%
175 epiboly) in epiboly were selected as hit compounds for in vitro testing using highly metastatic
176 human cancer cell lines. The study protocol was approved by the Institutional Animal Care
177 and Use Committee of the National University of Singapore (protocol number: R16-1068).
178
179 Reagents
180 FDA, EMA and other agencies approved chemical libraries was purchased from Prestwick
181 Chemical (Illkirch, France). Pizotifen and S(-) Eticlopride hydrochloride were purchased
182 from Sigma-Aldrich (St. Louis, MO).
183
184 Cell culture and cell viability assay
185 MCF7, MDA-MB-231, MDA-MB-435, MIA-PaCa2, PC3, SW620, PC9 and HaCaT cells
186 were obtained from American Type Culture Collection (ATCC, Manassas, VA). Luciferase-
187 expressing 4T1 (4T1-12B) cells were provided from Dr. Gary Sahagian (Tufts University,
188 Boston, MA). All culture methods followed the supplier's instruction. Cell viability assay
189 was performed as previously described (Nakayama et al., 2020).
190
191 Plasmid
192 A DNA fragment coding for HTR2C was amplified by PCR with primers containing
193 restriction enzyme recognition sequences. The HTR2C coding fragment was amplified from
194 hsp70l:mCherry-T2A-CreERT2 plasmid (11).
195
196 Immunoblotting

197 Western blotting was performed as described previously (Nakayama et al., 2020). Anti-
198 PRMT1, anti-CYP11A1, anti-E-cadherin, anti-EpCAM, anti-Vimentin, anti-N-cadherin, and
199 anti-GAPDH antibodies were purchased from Cell signaling Technology. Anti-HTR2C and
200 anti-DRD2 antibodies were purchased form Abcam.
201
202 Flow cytometry
203 Cells were stained with FITC-conjugated E-cadherin antibody (Biolegend, San Diego, CA).
204 Flow cytometry was performed as described (Nakayama et al., 2009) and analyzed with
205 FlowJo software (TreeStar, Ashland, OR).
206
207 shRNA mediated gene knockdown
208 The short hairpin RNA (shRNA)-expressing lentivirus vectors were
209 constructed using pLVX-shRNA1 vector (Clontech). PRMT1-shRNA_#3–targeting sequence
210 is GTGTTCCAGTATCTCTGATTA; PRMT1-shRNA_#4–targeting sequence is
211 TTGACTCCTACGCACACTTTG. CYP11A1-shRNA_#4–targeting sequence is
212 GCGATTCATTGATGCCATCTA; CYP11A1-shRNA_#4–targeting sequence is
213 GAAATCCAACACCTCAGCGAT. Human HTR2C-shRNA–targeting sequence is
214 TCATGCACCTCTGCGCTATAT. Mouse HTR2C-shRNA–targeting sequence is . LacZ-
215 shRNA– targeting sequence is CTACACAAATCAGCGATT.
216
217 Immunofluorescence
218 Immunofluorescence microscopy assay was performed by previously described (ref). Goat
219 anti-mouse and goat anti-rabbit immunoglobulin G (IgG) antibodies conjugated to Alexa
220 Fluor 488 (Life Technologies) and diluted at 1:100 were used. Nuclei were visualized by the

221 addition of 2μg/ml of 4', 6-diamidino-2-phenylindole (DAPI) and photographed at 100x
222 magnification by a fluorescent microscope (Zeiss, Germany).
223
224 Boyden chamber cell motility and invasion assay
225 These assays were performed by previously described (Nakayama et al., 2020). In Boyden
226 chamber assay, either 3x105 MDA-MB-231, 1x106 MDA-MB-435, or 5x105 PC9 cells were
227 applied to each well in the upper chamber.
228
229 Zebrafish xenotransplantation model
230 Tg(kdrl:eGFP) zebrafish was provided by Dr. Stainier (Max Planck Institute for Heart and
231 Lung Research). Embryos that were derived from the line were maintained in E3 medium
232 containing 200μM 1-phenyl-2-thiourea (PTU). Approximately 100-400 Red fluorescence
233 protein (RFP)-labelled MBA-MB-231 or MIA-Paca2 cells were injected into the duct of
234 Cuvier of the zebrafish at 2dpf. In this model, the dissemination patterns were generally
235 divided into three categories: (i) head dissemination, in which disseminated cells exist in the
236 vessel of the head part; (ii) trunk dissemination, in which the cells were observed in the
237 vessel dilating from the trunk to the tail; (iii) end-tail dissemination, in which the cells were
238 observed in the vessel of the end-tail part
239
240 Spontaneous metastasis mouse model
241 4T1-12B cells (2x104) were injected into the #4 mammary fat pad while the mice were
242 anesthetized. On day two post inoculation, the mice were randomly assigned to two groups
243 and one group received once daily intraperitoneal injections of 10mg/kg Pizotifen while the
244 other group received a vehicle injection. To monitor tumor growth and metastases, mice were
245 imaged biweekly by IVIS Imaging System (ParkinElmer). The primary tumor was resected

10 days after inoculation. The study protocol (protocol number: BRC IACUC #110612) was approved by A*STAR (Agency for Science, Technology and Research, Singapore).

Histological Analysis

All OCT embedded primary tumors, lungs, and livers of mice from the spontaneous metastasis 4T1 model were sectioned on a cryostat. Eight micron sections were taken at five hundred micron intervals through the entirety of the livers and lungs. Sections were subsequently stained with hematoxylin and eosin. Metastatic lesions were counted under a microscope in each section for both lungs and livers.

Statistics

Data were analyzed by Student's t test; $p < 0.05$ was considered significant.

References

1. Welch DR, Hurst DR. Defining the Hallmarks of Metastasis Cancer research. 2019;79(12):3011-27. .
2. Chaffer CL, Weinberg RA. A perspective on cancer cell metastasis Science. 2011;331(6024):1559-64.
3. Solnica-Krezel L. Conserved patterns of cell movements during vertebrate gastrulation Curr Biol. 2005;15(6):R213-28. .
4. Latimer A, Jessen JR. Extracellular matrix assembly and organization during zebrafish gastrulation. Matrix Biol. 2010;29(2):89-96.
5. Solnica-Krezel L. Gastrulation in zebrafish -- all just about adhesion? Curr Opin Genet Dev. 2006;16(4):433-41.
6. Tsai Y, Pan H, Hung C. The predominant protein arginine methyltransferase PRMT1 is critical for zebrafish convergence and extension during gastrulation. FEBS J. 2011;278(6):905-17.
7. Hsu J, Liang M, Chen C. Pregnenolone stabilizes microtubules and promotes zebrafish embryonic cell movement. Nature. 2006;439(7075):480-3.
8. Sack U, Walther W, Scudiero D. Novel effect of antihelminthic Niclosamide on S100A4-mediated metastatic progression in colon cancer. J Natl Cancer Inst. 2011;103(13):1018-36.
9. Huang E, Xue S, Zhang X. Vinpocetine inhibits breast cancer cells growth in vitro and in vivo. . Apoptosis. 2012;17(10):1120-30.
10. Nakayama J, Lu J, Makinoshima H, Gong Z. A Novel Zebrafish Model of Metastasis Identifies the HSD11β1 Inhibitor Adrenosterone as a Suppressor of Epithelial-

282 Mesenchymal Transition and Metastatic Dissemination Mol Cancer Res.
283 2020;18(3):477-87.
284 11. Kolosionek E, Savai R, Ghofrani HA. Expression and activity of phosphodiesterase
285 isoforms during epithelial mesenchymal transition: the role of phosphodiesterase 4 Mol
286 Biol Cell. 2009;20(22):4751-65.
287 12. Sasaki T, Kuniyasu H, Luo Y. Serum CD10 is associated with liver metastasis in
288 colorectal cancer J Surg Res. 2014;192(2):390-4.
289 13. Liu P, Kumar IS, Brown S, Kannappan V. Disulfiram targets cancer stem-like cells
290 and reverses resistance and cross-resistance in acquired paclitaxel-resistant triple-
291 negative breast cancer cells. Br J Cancer. 2013;109(7):1876-85.
292 14. Tao K, Fang M, Alroy J, Sahagian GG. Imagable 4T1 model for the study of late
293 stage breast cancer BMC Cancer. 2008;9(8):228.
294
295

Acknowledgments

We thank Drs. Joshua Collins (NIH/NIDCR) and Diane Palmieri (NIH/NCI) for helping this research, Dr. Herrick (Albany medical collage) for providing pCMV-h5TH2C-VSV with us. This study was funded by grants from National Medical Research Council of Singapore and Ministry of Education of Singapore.

Author Contributions

Design research; J.N. Conducting experiments; J.N. and L.T. Analyzing data: J.N. Writing the paper; J.N. and Z.G. Funding Acquisition; Z.G., S.W., B.C.G., H.M. and Supervision; Z.G.

Declaration of Interests

J.N., L.T., B.C.G., S.W., H.M. and Z.G. declare no conflict of interest.

309 **Figure 1**

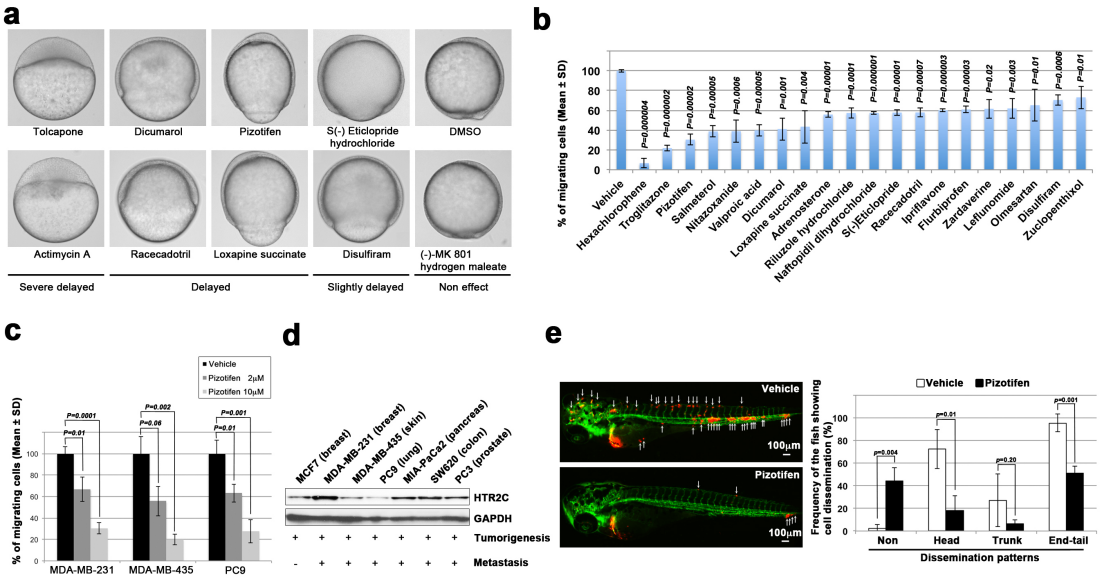

310

311 **Figure 1. A chemical screen for identification of epiboly-interrupting drugs.**

312 (A) Representative samples of the embryos that were treated with indicated drugs. (B) Effect
313 of the epiboly-interrupting drugs on cell motility and invasion of MDA-MB-231 cells
314 through Boyden chamber assays. (C) Effect of pizotifen on cell motility and invasion of
315 MDA-MB-231, MDA-MB-435 and PC9 cells through Boyden chamber assays. (D) Western
316 blot analysis of HTR2C levels in various human cancer cell lines with GAPDH as loading
317 control. (E) Representative images of dissemination of RFP-labelled MDA-MB-231 (231R)
318 cells in zebrafish xenotransplantation model. The fish that were inoculated with 231R cells,
319 were treated with either vehicle or Pizotifen. Arrows indicate disseminated 231R cells. The
320 mean frequencies of the fish showing head, trunk, or end-tail dissemination were counted
321 (right). Each value is indicated as the mean±SEM of two independent experiments. Statistical
322 analysis was determined by Student's t test.

323 **Figure 2**

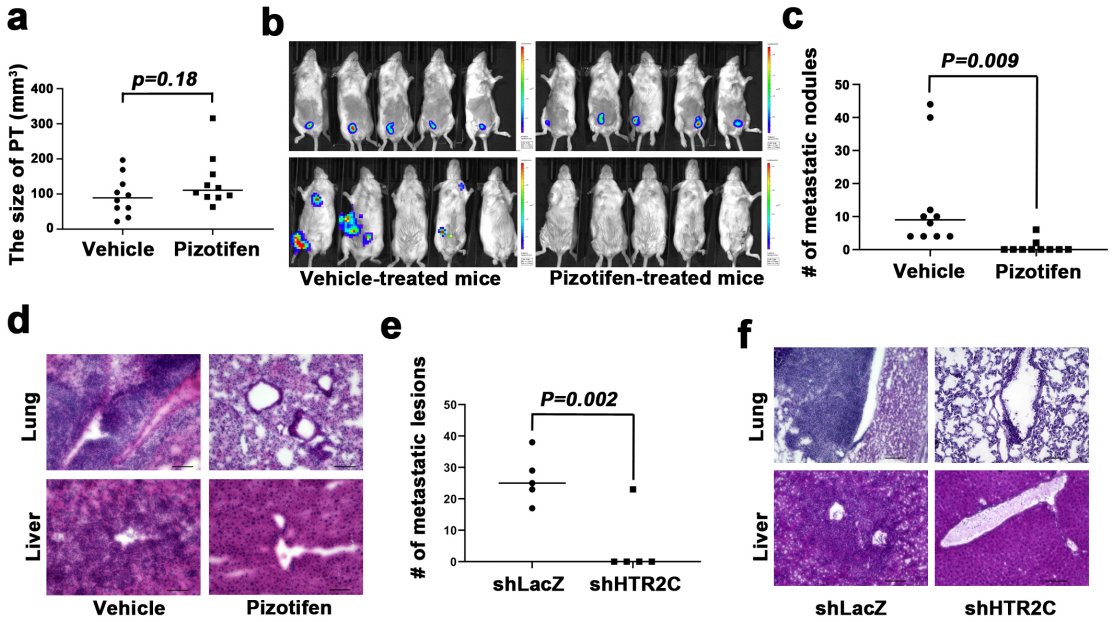

324

325 **Figure 2. Epiboly-interrupting drugs suppressed metastatic progression in a mouse**

326 **metastasis model .**

327 (A) Mean volumes (n=10 per group) of 4T1 primary tumors formed in MFP of either vehicle

328 or Pizotifen-treated mice at day 10 post-injection. (B) Representative images of primary

329 tumors on day 10 post-injection (top) and metastatic burden on day 70 post-injection

330 (bottom). (C) Number of metastatic nodules in the lung of either vehicle or Pizotifen-treated

331 mice. (D) Representative H&E staining of the lung (top) and liver (bottom) from either

332 vehicle or Pizotifen-treated mice. (E) The mean number of metastatic lesions in step sections

333 of the lungs from the mice that were inoculated with either shLacZ or shHTR2C_4T1 cells.

334 (F) Representative H&E staining of the lung and liver from the mice that were inoculated

335 with 4T1 cells expressing shRNA targeting for either LacZ or HTR2C. Each value is

336 indicated as the mean±SEM. Statistical analysis was determined by Student's *t* test.

337 **Supplementary Figure 1**

338

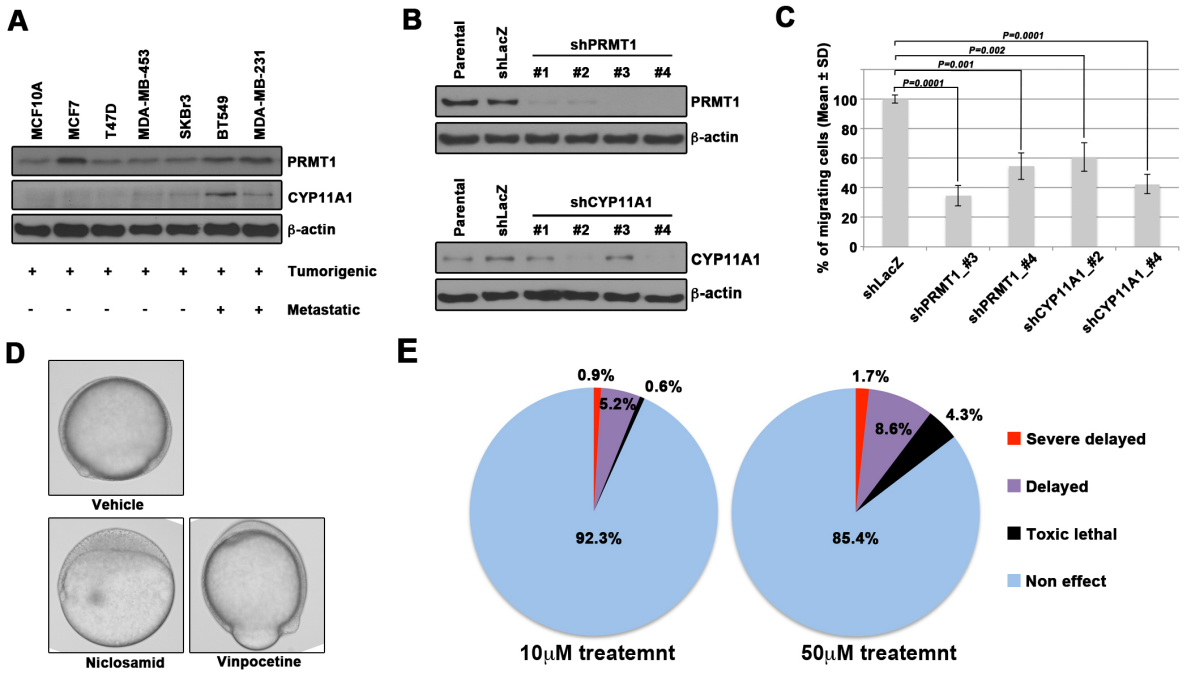

339
340
341

342 **Supplementary Figure 1. Molecular mechanisms of epiboly in zebrafish overlap with**

343 **those in cancer metastasis.**

344 (A) Western blot analysis of PRMT1 (upper) and CYP11A1 (middle) protein levels in non-

345 metastatic human cancer cell lines, (MCF10, MCF7, MDA-MB-453, Sun159, SKBr3) and

346 highly metastatic human cancer cell lines, (BT549 and MDA-MB-231); β-actin loading

347 control is shown (bottom). (B) Knockdown of PRMT1 or CYP11A1 in MDA-MB-231 cells.

348 MBA-MB-231 cells were transfected with a control shRNA targeting LacZ, and one of four

349 independent shRNAs targeting PRMT1 (clone #1 to #4) or one of two independent shRNAs

350 targeting CYP11A1 (clone #1 to #4). Reduced PRMT1 and CYP11A1 expression,

351 determined by western blot, in sub-cell lines of MDA-MB-231 cells expressing PRMT1

352 shRNA (clone #3 and #4 or CYP11A1 (clone #2 and #4), compared with controls (parental

353 cell line MDA-MB-231 and control shRNA cells); β-actin levels shown as a loading control.

354 (C) Effect of shRNAs targeting either PRMT1 or CYP11A1 on cell motility and invasion of

355 MBA-MB-231 cells. Parental MDA-MB-231 cells and four sub-cell lines of MDA-MB-231

356 cells that were transfected with either shRNA targeting either LacZ, two independent
357 shRNAs targeting PRMT1 (clone #3 and #4) or two independent shRNAs targeting
358 CYP11A1 (clone #2 and #4), were subjected to Boyden chamber assays. (D) Zebrafish
359 embryos treated with either vehicle (DMSO), 10μM Niclosamide, or 50μM vinpocetine.
360 Approximately 20 embryos were treated with either DMSO as a vehicle control, niclosamide,
361 or vinpocetine. The treatment was started at 4 hpf when all of embryos reached sphere stage
362 and ended at 9 hpf when control embryos reached 80-90% epiboly stage. Each experiment
363 was performed at least twice. Statistical analysis was determined by Student's *t* test. (E)
364 Cumulative results of the chemical screen in which each drug was used at either 10μM (left) or
365 50μM (right) concentrations. 1,280 FDA, EMA or other agencies-approved drugs were subjected
366 to this screening. Positive "hit" drugs were those that interrupted epiboly progression.
367

368
369 **Supplementary Figure 2**

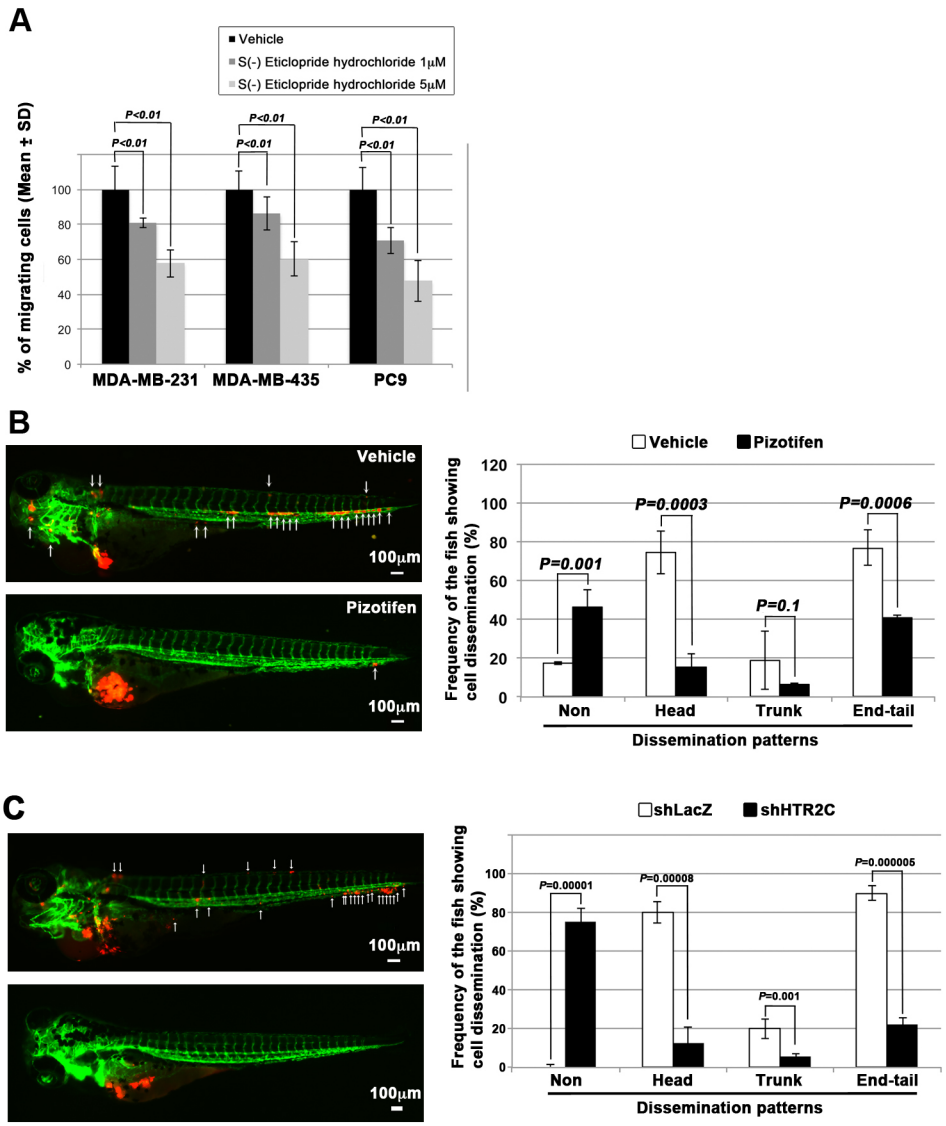

370

371 **Supplementary Figure 2. Epiboly-interrupting drugs suppressed metastatic dissemination**

372 **of human cancer cells in a zebrafish xenotransplantation model.**

373 (A) Effect of S (-) Eticlopride hydrochloride on cell motility and invasion of MBA-MB-231,

374 MDA-MB-435, and PC9 cells. Either vehicle or pizotifen treated cells were subjected to Boyden

375 chamber assays. Fetal bovine serum (1%v/v) was used as the chemoattractant in both assays.

376 Each experiment was performed at least twice. Statistical analysis was determined by Student's *t*

377 test. (B) and (C) Representative images of dissemination of RFP-labelled MIA-PaCa2, RFP-

378 labelled MDA-MB-231 cells expressing shRNA targeting either LacZ (shLacZ_231R) or HTR2C

379 (shHTR2C_231R) cells in zebrafish xenotransplantation model. The fish larvae that were
380 inoculated with RFP-labelled MIA-PaCa2 cells, were treated with either vehicle (top) or the drug
381 (lower) (B). The fish larvae that were inoculated with either shLacZ_231R (top) or
382 shHTR2C_231R cells (lower) (C). Arrows indicate disseminated RFP-labelled MIA-PaCa2 or
383 231R cells. The images were shown in 4x magnification. Scale bar, 100μm. The mean
384 frequencies of the fish showing head, trunk, or end-tail dissemination were counted (graph on
385 right). Each value is indicated as the mean ± SEM of two independent experiments. Statistical
386 analysis was determined by Student's t test.
387
388

389 **Supplementary Figure 3**

390

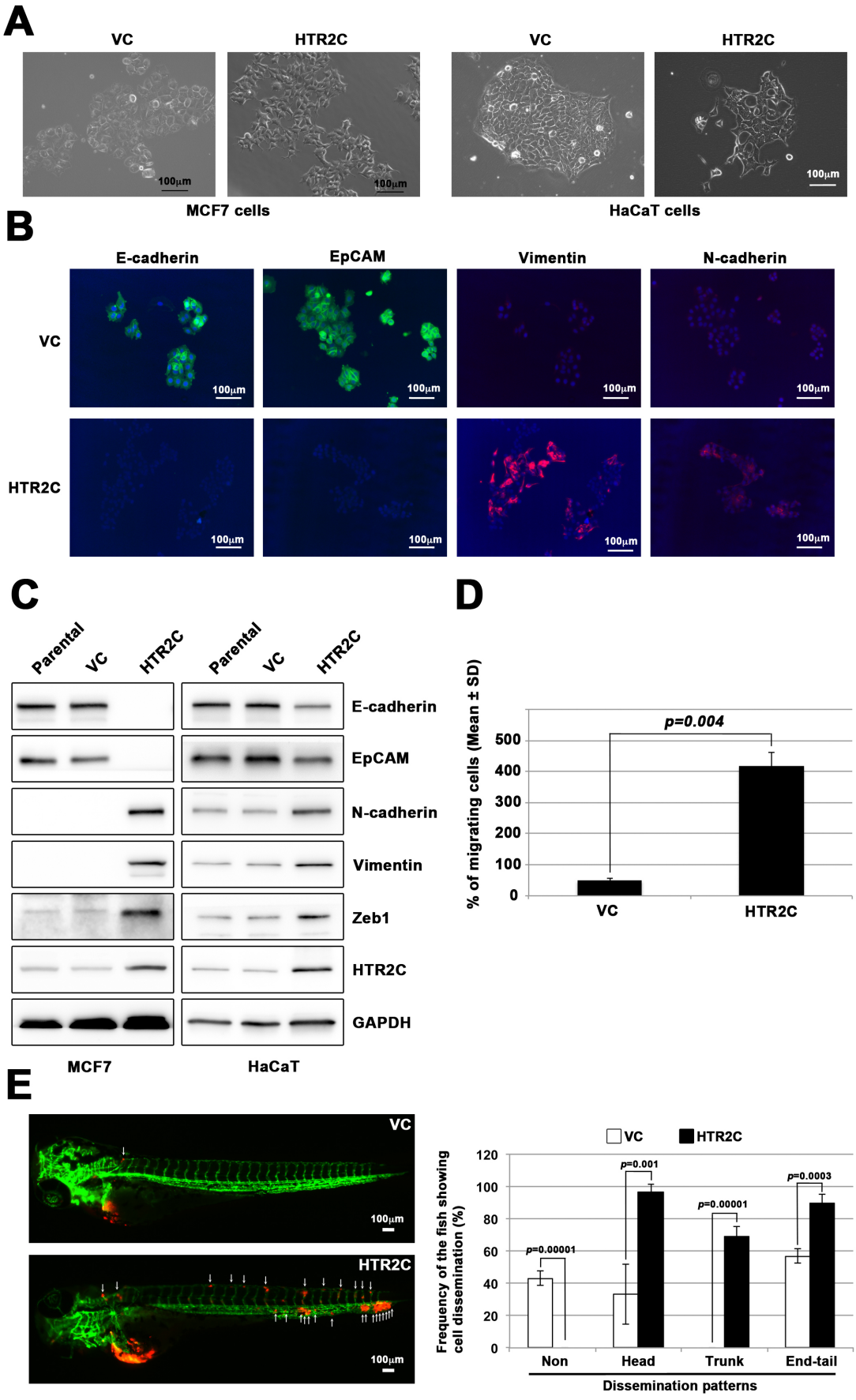

391

392 **Supplementary Figure 3. HTR2C induced EMT-mediated metastatic dissemination of**
393 **human cancer cells.**
394 (A) The morphologies of the MCF7 and HaCaT cells expressing either the control vector or
395 HTR2C were revealed by phase contrast microscopy. (B) Immunofluorescence staining of E-
396 cadherin, EpCAM, Vimentin, and N-cadherin expressions in the MCF7 cells from
397 Supplementary Figure 3A. (C) Expression of E-cadherin, EpCAM, Vimentin, N-cadherin, and
398 HTR2C was examined by western-blotting in the MCF7 and HaCaT cells; GAPDH loading
399 control is shown (bottom). (D) Effect of HTR2C on cell motility and invasion of MCF7 cells.
400 MCF7 cells were subjected to Boyden chamber assays. Fetal bovine serum (1%v/v) was used as
401 the chemoattractant in both assays. Each experiment was performed at least twice. (E)
402 Representative images of dissemination patterns of MCF7 cells expressing either the control
403 vector (top left) or HTR2C (lower left) in a zebrafish xenotransplantation model. White arrows
404 head indicate disseminated MCF7 cells. The mean frequencies of the fish showing head, trunk, or
405 end-tail dissemination tabulated (right). Each value is indicated as the mean ± SEM of two
406 independent experiments. Statistical analysis was determined by Student's *t* test.
407

408 **Supplementary Table 1. A list of the genes that are involved between gastrulation and**
409 **metastasis progression**
410

Genes	Gastrulation Defects	Ref	Effects in Metastasis	Ref
BMP	Convergence and extension	(1)	EMT	(2)
WNT	Convergence and extension	(3)	Migration and Invasion	(4)
FGF	Convergence and extension	(5)	Invision	(6)
EGF	Epiboly	(7)	Migration	(8)
PDGF	Convergence and extension	(9)	EMT	(10)
CXCL12	Migration of endodermal cells	(11)	Migration and Invasion	(12)
CXCR4	Migration of endodermal cells	(11)	Migration and Invasion	(12)
PIK3CA	Convergence and extension	(13)	Migration and Invasion	(14)
YES	Epiboly	(15)	Migration	(16)
FYN	Epiboly	(17)	Migration and Invasion	(18)
MAPK1	Epiboly	(19)	Migration	(20)
SHP2	Convergence and extension	(21)	Migration	(22)
SNAI1	Convergence and extension	(23)	EMT	(24)
SNAI2	Mesoderm & Neural crest formation	(25)	EMT	(24)
TWIST1	Mesoderm formation	(26)	EMT	(27)
TBXT	Convergence and extension	(3)	EMT	(28)
ZEB1	Epiboly	(29)	EMT	(30)
GSC	Mesodermal patterning	(31)	EMT	(32)
FOXC2	Unclear, defects in gastrulation	(33)	EMT	(34)
STAT3	Convergence and extension	(35)	Migration	(36)
POU5F1	Epiboly	(37)	EMT	(38)
EZH2	Unclear, defects in gastrulation	(39)	Invasion	(40)
EHMT2	Defects in Neurogenesis	(41)	Migration and Invasion	(42)
BMI1	Defects in skelton formation	(43)	EMT	(44)
RHOA	Convergence and extension	(45)	Migration and Invasion	(46)
CDC42	Convergence and extension	(47)	Migration and Invasion	(48)
RAC1	Convergence and extension	(49)	Migration and Invasion	(50)
ROCK2	Convergence and extension	(51)	Migration and Invasion	(52)
PAR1	Convergence and extension	(53)	Migration	(54)
PRKCI	Convergence and extension	(53)	EMT	(55)
CAP1	Convergence and extension	(56)	Migration	(57)
EZR	Epiboly	(58)	Migration	(59)
EPCAM	Epiboly	(60)	Migration and Invasion	(61)
ITGB1 / ITA5	Mesodermal Migration	(62)	Migration and Invasion	(63)
FN1	Convergence and extension	(64)	Invasion	(65)
HAS2	Dorsal migration of lateral cells	(66)	Invasion	(67)
MMP14	Convergence and extension	(68)	Invasion	(69)
COX1	Epiboly	(70)	Invasion	(71)
PTGES	Convergence and extension	(72)	Invasion	(73)
SLC39A6	Aterior migration	(74)	EMT	(75)
GNA12 / 13	Convergence and extension	(41)	Migration and Invasion	(76)
OGT	Epiboly	(77)	Migration and Invasion	(78)
CCN1	Cell Movement	(79)	Migration and Invasion	(80)
TRPM7	Convergence and extension	(81)	Migration	(82)
MAPKAPK2	Epiboly	(83)	Migration	(84)
B4GALT1	Convergence and extension	(85)	Invasion	(86)
IER2	Convergence and extension	(87)	Migration	(88)
TIP1	Convergence and extension	(89)	Migration and Invasion	(90)
PAK5	Convergence and extension	(91)	Migration	(92)
MARCKS	Convergence and extension	(93)	Migration and Invasion	(94)

411
412 **Supplementary Table 1.**

413 A list of the fifty genes that play essential role in governing both metastasis and gastrulation
414 progression. The gastrulation defects in Xenopus or zebrafish that are induced by knockdown

415 of each of these genes, were indicated. The molecular mechanism in metastasis that are

416 inhibited by knockdown of each of the same genes, were indicated.

417 **Supplementary Table 2. A list of the drugs that interfere with epiboly progression in**
418 **zebrafish**
419

Chemical name	Chemical formula	Effect of 10uM	Effect of 50uM
Acitretin	C21H26O3	Delayed	Delayed
Adrenosterone	C19H24O3	Delayed	Delayed
Albendazole	C12H15N3O2S	Severe delayed	Severe delayed
Alfadolone acetate	C23H34O5	Delayed	Delayed
Alfaxalone	C21H32O3	Delayed	Delayed
Alprostadil	C20H34O5	Delayed	Delayed
Altrenogest	C21H26O2	Slightly delayed	Delayed
Ampiroxicam	C20H21N3O7S	Non effect	Delayed
Anethole-trithione	C10H8OS3	Delayed	Delayed
Antimycin A	C28H40N2O9	Delayed	Delayed
Avobenzone	C20H22O3	Delayed	Delayed
Benzoxiquine	C16H11NO2	Non effect	Delayed
Bosentan	C27H29N5O6S	Delayed	Delayed
Butoconazole nitrate	C19H18Cl3N3O3S	Delayed	Toxic lethal
Camptothecine (S,+)	C20H16N2O4	Severe delayed	Severe delayed
Carbenoxolone disodium salt	C34H48Na2O7	Delayed	Toxic lethal
Carmofur	C11H16FN3O3	Slightly delayed	Delayed
Carprofen	C15H12ClNO2	Severe delayed	Toxic lethal
Cefdinir	C14H13N5O5S2	Delayed	Delayed
Celecoxib	C17H14F3N3O2S	Delayed	Delayed
Chlorambucil	C14H19Cl2NO2	Slightly delayed	Delayed
Chlorhexidine	C22H30Cl2N10	Non effect	Toxic lethal
Ciclopirox ethanolamine	C14H24N2O3	Delayed	Severe delayed
Cinoxacin	C12H10N2O5	Delayed	Severe delayed
Clofibrate	C12H15ClO3	Non effect	Severe delayed
Clopidogrel	C16H16ClNO2S	Non effect	Delayed
Clorgyline hydrochloride	C13H16Cl3NO	Delayed	Delayed
Colchicine	C22H25NO6	Non effect	Delayed
Deptropine citrate	C29H35NO8	Delayed	Delayed
Desipramine hydrochloride	C18H23ClN2	Delayed	Delayed
Diclofenac sodium	C14H10Cl2NNaO2	Delayed	Severe delayed
Dicumarol	C19H12O6	Delayed	Severe delayed
Diethylstilbestrol	C18H20O2	Delayed	Toxic lethal
Dimaprit dihydrochloride	C6H17Cl2N3S	Slightly delayed	Delayed
Disulfiram	C10H20N2S4	Delayed	Delayed
Dopamine hydrochloride	C8H12ClNO2	Delayed	Delayed
Eburnamonine (-)	C19H22N2O	Delayed	Delayed
Ethaverine hydrochloride	C24H30ClNO4	Delayed	Delayed
Ethinylestradiol	C20H24O2	Delayed	Severe delayed
Ethopropazine hydrochloride	C19H25ClN2S	Delayed	Delayed
Ethoxyquin	C14H19NO	Non effect	Delayed
Exemestane	C20H24O2	Slightly delayed	Delayed
Ezetimibe	C24H21F2NO3	Slightly delayed	Delayed
Fenbendazole	C15H13N3O2S	Non effect	Delayed
Fenoprofen calcium salt dihydrate	C30H30CaO8	Slightly delayed	Delayed
Fentiazac	C17H12ClNO2S	Toxic lethal	Toxic lethal
Floxuridine	C9H11FN2O5	Delayed	Toxic lethal
Flunixin meglumine	C21H28F3N3O7	Delayed	Toxic lethal
Flutamide	C11H11F3N2O3	Delayed	Toxic lethal
Fluticasone propionate	C25H31F3O5S	Non effect	Delayed
Furosemide	C12H11ClN2O5S	Delayed	Delayed
Gatifloxacin	C19H22FN3O4	Delayed	Delayed
Gemcitabine	C9H11F2N3O4	Delayed	Delayed
Gemfibrozil	C15H22O3	Delayed	Toxic lethal
Gestrinone	C21H24O2	Delayed	Delayed
Haloprogin	C9H4Cl3IO	Delayed	Toxic lethal
Hexachlorophene	C13H6Cl6O2	Delayed	Severe delayed
Hexestrol	C18H22O2	Slightly delayed	Delayed
Ibudilast	C14H18N2O	Non effect	Delayed

Idazoxan hydrochloride	C11H13ClN2O2	Slightly delayed	Delayed
Idazoxan hydrochloride	C11H13ClN2O2	Non effect	Delayed
Idebenone	C19H30O5	Severe delayed	Toxic lethal
Indomethacin	C19H16ClNO4	Non effect	Delayed
Ipriflavone	C18H16O3	Delayed	Severe delayed
Isotretinoin	C20H28O2	Non effect	Severe delayed
Isradipine	C19H21N3O5	Non effect	Delayed
Lansoprazole	C16H14F3N3O2S	Slightly delayed	Delayed
Latanoprost	C26H40O5	Non effect	Delayed
Leflunomide	C12H9F3N2O2	Delayed	Severe delayed
Letrozole	C17H11N5	Non effect	Delayed
Lithocholic acid	C24H40O3	Non effect	Delayed
Lodoxamide	C11H6ClN3O6	Non effect	Delayed
Lofepramine	C26H27ClN2O	Non effect	Delayed
Loratadine	C22H23ClN2O2	Delayed	Delayed
Loxapine succinate	C22H24ClN3O5	Delayed	Delayed
Mebendazole	C16H13N3O3	Severe delayed	Severe delayed
Mebendazole	C22H26N2O2	Non effect	Delayed
Meloxicam	C14H13N3O4S2	Delayed	Toxic lethal
Methiazole	C12H15N3O2S	Delayed	Delayed
Mevastatin	C23H34O5	Non effect	Delayed
MK 801 hydrogen maleate	C20H19NO4	Slightly delayed	Delayed
Nabumetone	C15H16O2	Non effect	Severe delayed
Naftopidil dihydrochloride	C24H30Cl2N2O3	Slightly delayed	Delayed
Nandrolone	C18H26O2	Delayed	Delayed
Naproxen sodium salt	C14H13NaO3	Delayed	Delayed
Niclosamide	C13H8Cl2N2O4	Delayed	Delayed
Nifekalant	C19H27N5O5	Delayed	Delayed
Niflumic acid	C13H9F3N2O2	Delayed	Delayed
Nimesulide	C13H12N2O5S	Non effect	Delayed
Nisoldipine	C20H24N2O6	Delayed	Toxic lethal
Nitazoxanide	C12H9N3O5S	Severe delayed	Severe delayed
Norethindrone	C20H26O2	Non effect	Delayed
Norgestimate	C23H31NO3	Slightly delayed	Delayed
Oxfendazol	C15H13N3O3S	Slightly delayed	Delayed
Oxibendazol	C12H15N3O3	Severe delayed	Severe delayed
Oxymetholone	C21H32O3	Slightly delayed	Delayed
Parbendazole	C13H17N3O2	Severe delayed	Severe delayed
Parthenolide	C15H20O3	Non effect	Delayed
Penciclovir	C10H15N5O3	Non effect	Delayed
Pentobarbital	C11H18N2O3	Non effect	Delayed
Phenazopyridine hydrochloride	C11H12ClN5	Delayed	Toxic lethal
Phenothiazine	C12H9NS	Non effect	Delayed
Phenoxybenzamine hydrochloride	C18H23Cl2NO	Non effect	Delayed
Pizotifen malate	C23H27NO5S	Delayed	Severe delayed
Pramoxine hydrochloride	C17H28ClNO3	Slightly delayed	Delayed
Prilocaine hydrochloride	C13H21ClN2O	Non effect	Delayed
Primidone	C12H14N2O2	Slightly delayed	Delayed
Racecadotril	C21H23NO4S	Slightly delayed	Delayed
Riluzole hydrochloride	C8H6ClF3N2OS	Non effect	Delayed
Ritonavir	C37H48N6O5S2	Non effect	Severe delayed
S(-)Eticlopride hydrochloride	C17H26Cl2N2O3	Delayed	Delayed
Salmeterol	C25H37NO4	Non effect	Delayed
Streptomycin sulfate	C42H84N14O36S3	Non effect	Delayed
Sulconazole nitrate	C18H16Cl3N3O3S	Delayed	Delayed
Tegafur	C8H9FN2O3	Delayed	Delayed
Telmisartan	C33H30N4O2	Severe delayed	Toxic lethal
Tenatoprazole	C16H18N4O3S	Non effect	Delayed
Terbinafine	C21H25N	Non effect	Delayed
Thimerosal	C9H9HgNaO2S	Non effect	Delayed
Thiorphan	C12H15NO3S	Delayed	Delayed
Tolcapone	C14H11NO5	Severe delayed	Severe delayed
Topotecan	C23H23N3O5	Delayed	Delayed
Tracazolate hydrochloride	C16H25ClN4O2	Severe delayed	Delayed

Tribenoside	C29H34O6	Delayed	Delayed
Triclabendazole	C14H9Cl3N2OS	Delayed	Delayed
Triclosan	C12H7Cl3O2	Delayed	Severe delayed
Trioxsalen	C14H12O3	Delayed	Delayed
Troglitazone	C24H27NO5S	Severe delayed	Toxic lethal
Valproic acid	C8H16O2	Non effect	Delayed
Voriconazole	C16H14F3N5O	Non effect	Delayed
Zardaverine	C12H10F2N2O3	Slightly delayed	Delayed
Zuclopenthixol dihydrochloride	C22H27Cl3N2OS	Delayed	Delayed

Supplementary Table 2. A list of the drugs that interfere with epiboly progression in zebrafish

A list of positive "hit" drugs that interfered with epiboly progression. Gastrulation defects or status of each of the zebrafish embryos that were treated with either 10μM or 50μM concentrations, are indicated.

427 **Supplementary Table 3. Primary targets of the identified drugs**

428

The identified drugs	Primary targets of the identified drugs
Hexachlorophene	D-lactate dehydrogenase (D-LDH), not expressed in mammalian cells
Troglitazone	Agonist for Peroxisome proliferator-activated receptor α and γ (PPARα and γ)
Pizotifen malate	5-hydroxytryptamine receptor 2C (HTR2C)
Salmeterol	Adrenergic receptor beta 2 (ADRB2)
Nitazoxanide	Pyruvate ferredoxin oxidoreductase (PFOR), not expressed in mammalian cells
Valproic acid	Histone deacetylases (HDACs)
Dicumarol	NAD(P)H dehydrogenase quinone 1 (NQO1)
Loxapine succinate	Dopamine receptor D2 and D4 (DRD2 and DRD4)
Adrenosterone	Hydroxysteroid (11-beta) dehydrogenase 1 (HSD11β1)
Riluzole hydrochloride	Glutamate R and Voltage-dependent Na+ channel
Naftopidil dihydrochloride	5-hydroxytryptamine receptor 1A (HTR1A) and α1-adrenergic receptor (AR)
S(-)Eticlopride hydrochloride	Dopamine receptor D2 (DRD2)
Racecadotril	Membrane metallo-endopeptidase (MME)
Ipriflavone	Unknow
Flurbiprofen	Cyclooxygenase 1 and 2 (Cox1 and 2)
Zardaverine	Phosphodiesterase III/IV (PDE3/4)
Leflunomide	Dihydroorotate dehydrogenase (DHODH)
Olmesartan	Angiotensin II receptor alpha
Disulfiram	Aldehyde dehydrogenase (ALDH) Dopamine β-hydroxylase (DBH)
Zuclopenthixol dihydrochloride	Dopamine receptors D1 and D2 (DRD1 and 2)

429

430

References for supplemental table 1

1. Kondo M. Bone morphogenetic proteins in the early development of zebrafish. FEBS J. 2007;274(12):2960-7.
2. Katsuno Y, Hanyu A, Kanda H, Ishikawa Y, Akiyama F, Iwase T, et al. Bone morphogenetic protein signaling enhances invasion and bone metastasis of breast cancer cells through Smad pathway. Oncogene. 2008;27(49):6322-33.
3. Tada M, Smith JC. Xwnt11 is a target of Xenopus Brachyury: regulation of gastrulation movements via Dishevelled, but not through the canonical Wnt pathway. Development. 2000;127:2227-38.
4. Vincan E, Barker N. The upstream components of the Wnt signalling pathway in the dynamic EMT and MET associated with colorectal cancer progression. Clin Exp Metastasis. 2008;25(6):657-63.
5. Yang X, Dormann D, Munsterberg AE, Weijer CJ. Cell movement patterns during gastrulation in the chick are controlled by positive and negative chemotaxis mediated by FGF4 and FGF8. Dev Cell. 2002;3(3):425-37.
6. Nomura S, Yoshitomi H, Takano S, Shida T, Kobayashi S, Ohtsuka M, et al. FGF10/FGFR2 signal induces cell migration and invasion in pancreatic cancer. Br J Cancer. 2008;99(2):305-13.
7. Song S, Eckerle S, Onichtchouk D, Marrs JA, Nitschke R, Driever W. Pou5f1-dependent EGF expression controls E-cadherin endocytosis, cell adhesion, and zebrafish epiboly movements. Dev Cell. 2013;24(5):486-501.
8. Lu Z, Jiang G, Blume-Jensen P, Hunter T. Epidermal growth factor-induced tumor cell invasion and metastasis initiated by dephosphorylation and downregulation of focal adhesion kinase. Mol Cell Biol. 2001;21(12):4016-31.
9. Damm EW, Winklbauer R. PDGF-A controls mesoderm cell orientation and radial intercalation during Xenopus gastrulation. Development. 2011;138(3):565-75.
10. Jechlinger M, Sommer A, Moriggl R, Seither P, Kraut N, Capodiecci P, et al. Autocrine PDGFR signaling promotes mammary cancer metastasis. J Clin Invest. 2006;116(6):1561-70.
11. Mizoguchi T, Verkade H, Heath JK, Kuroiwa A, Kikuchi Y. Sdf1/Cxcr4 signaling controls the dorsal migration of endodermal cells during zebrafish gastrulation. Development. 2008;135(15):2521-9.
12. Shen HB, Gu ZQ, Jian K, Qi J. CXCR4-mediated Stat3 activation is essential for CXCL12-induced cell invasion in bladder cancer. Tumour Biol. 2013;34(3):1839-45.
13. Montero J-A, Kilian B, Chan J, Bayliss PE, Heisenberg C-P. Phosphoinositide 3-Kinase Is Required for Process Outgrowth and Cell Polarization of Gastrulating Mesendodermal Cells. Current Biology. 2003;13(15):1279-89.
14. Wander SA, Zhao D, Besser AH, Hong F, Wei J, Ince TA, et al. PI3K/mTOR inhibition can impair tumor invasion and metastasis in vivo despite a lack of antiproliferative action in vitro: implications for targeted therapy. Breast Cancer Res Treat. 2013;138(2):369-81.
15. Tsai WB, Zhang X, Sharma D, Wu W, Kinsey WH. Role of Yes kinase during early zebrafish development. Dev Biol. 2005;277(1):129-41.
16. Barraclough J, Hodgkinson C, Hogg A, Dive C, Welman A. Increases in c-Yes Expression Level and Activity Promote Motility But Not Proliferation of Human Colorectal Carcinoma Cells. Neoplasia. 2007;9(9):745-IN32.

480 17. Sharma D, Holets L, Zhang X, Kinsey WH. Role of Fyn kinase in signaling
481 associated with epiboly during zebrafish development. Dev Biol.
482 2005;285(2):462-76.
483 18. Yadav V, Denning MF. Fyn is induced by Ras/PI3K/Akt signaling and is
484 required for enhanced invasion/migration. Mol Carcinog. 2011;50(5):346-52.
485 19. Krens SF, He S, Lamers GE, Meijer AH, Bakkers J, Schmidt T, et al. Distinct
486 functions for ERK1 and ERK2 in cell migration processes during zebrafish
487 gastrulation. Dev Biol. 2008;319(2):370-83.
488 20. Radtke S, Milanovic M, Rossé C. ERK2 but not ERK1 mediates HGF-
489 induced motility in non-small cell lung carcinoma cell lines. J Cell Sci.
490 2013;126(Pt11):2381-91.
491 21. Jopling C, van Geemen D, den Hertog J. Shp2 knockdown and
492 Noonan/LEOPARD mutant Shp2-induced gastrulation defects. PLoS Genet.
493 2007;3(12):e225.
494 22. Wang FM, Liu HQ, Liu SR, Tang SP, Yang L, Feng GS. SHP-2 promoting
495 migration and metastasis of MCF-7 with loss of E-cadherin, dephosphorylation of
496 FAK and secretion of MMP-9 induced by IL-1beta in vivo and in vitro. Breast
497 Cancer Res Treat. 2005;89(1):5-14.
498 23. Ip YT, Gridley T. Cell movements during gastrulation: snail dependent and
499 independent pathways. Curr Opin Genet Dev. 2002;12(4):423-9.
500 24. Batlle E, Sancho E, Francí C, Domínguez D, Monfar M. The transcription
501 factor snail is a repressor of E-cadherin gene expression in epithelial tumour
502 cells. Nat Cell Biol. 2000;2(2):84-9.
503 25. Shi J, Severson C, Yang J, Wedlich D, Klymkowsky MW. Snail2 controls
504 mesodermal BMP/Wnt induction of neural crest. Development.
505 2011;138(15):3135-45.
506 26. Castanon I, Baylies MK. A Twist in fate: evolutionary comparison of Twist
507 structure and function. Gene. 2002;287(1-2):11-22.
508 27. Yang J, Mani SA, Donaher JL, Ramaswamy S, Itzykson RA, Come C, et al.
509 Twist, a master regulator of morphogenesis, plays an essential role in tumor
510 metastasis. Cell. 2004;117(7):927-39.
511 28. Fernando RI, Litzinger M, Trono P, Hamilton DH, Schlom J, Palena C. The
512 T-box transcription factor Brachyury promotes epithelial-mesenchymal
513 transition in human tumor cells. J Clin Invest. 2010;120(2):533-44.
514 29. Vannier C, Mock K, Brabletz T, Driever W. Zeb1 regulates E-cadherin and
515 Epcam (epithelial cell adhesion molecule) expression to control cell behavior in
516 early zebrafish development. J Biol Chem. 2013;288(26):18643-59.
517 30. Spaderna S, Schmalhofer O, Wahlbuhl M, Dimmler A, Bauer K, Sultan A, et
518 al. The transcriptional repressor ZEB1 promotes metastasis and loss of cell
519 polarity in cancer. Cancer Res. 2008;68(2):537-44.
520 31. Sander V, Reversade B, De Robertis EM. The opposing homeobox genes
521 Goosecoid and Vent1/2 self-regulate Xenopus patterning. EMBO J.
522 2007;26(12):2955-65.
523 32. Hartwell KA, Muir B, Reinhardt F, Carpenter AE, Sgroi DC, Weinberg RA.
524 The Spemann organizer gene, Goosecoid, promotes tumor metastasis. Proc Natl
525 Acad Sci U S A. 2006;103(50):18969-74.
526 33. Wilm B, James RG, Schultheiss TM, Hogan BL. The forkhead genes, Foxc1
527 and Foxc2, regulate paraxial versus intermediate mesoderm cell fate. Dev Biol.
528 2004;271(1):176-89.
529 34. Mani SA, Yang J, Brooks M, Schwaninger G, Zhou A, Miura N, et al.
530 Mesenchyme Forkhead 1 (FOXC2) plays a key role in metastasis and is associated

531 with aggressive basal-like breast cancers. Proc Natl Acad Sci U S A.
532 2007;104(24):10069-74.
533 35. Miyagi C, Yamashita S, Ohba Y, Yoshizaki H, Matsuda M, Hirano T. STAT3
534 noncell-autonomously controls planar cell polarity during zebrafish convergence
535 and extension. J Cell Biol. 2004;166(7):975-81.
536 36. Abdulghani J, Gu L, Dagvadorj A, Lutz J, Leiby B, Bonuccelli G, et al. Stat3
537 promotes metastatic progression of prostate cancer. Am J Pathol.
538 2008;172(6):1717-28.
539 37. Lachnit M, Kur E, Driever W. Alterations of the cytoskeleton in all three
540 embryonic lineages contribute to the epiboly defect of Pou5f1/Oct4 deficient
541 MZspg zebrafish embryos. Dev Biol. 2008;315(1):1-17.
542 38. Dai X, Ge J, Wang X, Qian X, Zhang C, Li X. OCT4 regulates epithelial-
543 mesenchymal transition and its knockdown inhibits colorectal cancer cell
544 migration and invasion. Oncol Rep. 2013;29(1):155-60.
545 39. O'Carroll D, Erhardt S, Pagani M, Barton SC, Surani MA, Jenuwein T. The
546 polycomb-group gene Ezh2 is required for early mouse development. Mol Cell
547 Biol. 2001;21(13):4330-6.
548 40. Ren G, Baritaki S, Marathe H, Feng J, Park S, Beach S, et al. Polycomb
549 protein EZH2 regulates tumor invasion via the transcriptional repression of the
550 metastasis suppressor RKIP in breast and prostate cancer. Cancer Res.
551 2012;72(12):3091-104.
552 41. Lin F, Sepich DS, Chen S, Topczewski J, Yin C, Solnica-Krezel L, et al.
553 Essential roles of G{alpha}12/13 signaling in distinct cell behaviors driving
554 zebrafish convergence and extension gastrulation movements. J Cell Biol.
555 2005;169(5):777-87.
556 42. Chen MW, Hua KT, Kao HJ, Chi CC, Wei LH, Johansson G, et al. H3K9
557 histone methyltransferase G9a promotes lung cancer invasion and metastasis by
558 silencing the cell adhesion molecule Ep-CAM. Cancer Res. 2010;70(20):7830-40.
559 43. van der Lugt NM, Domen J, Linders K, van Roon M, Robanus-Maandag E, te
560 Riele H, et al. Posterior transformation, neurological abnormalities, and severe
561 hematopoietic defects in mice with a targeted deletion of the bmi-1 proto-
562 oncogene. Genes Dev. 1994;8(7):757-69.
563 44. Guo BH, Feng Y, Zhang R, Xu LH, Li MZ, Kung HF, et al. Bmi-1 promotes
564 invasion and metastasis, and its elevated expression is correlated with an
565 advanced stage of breast cancer. Mol Cancer. 2011;10(1):10.
566 45. Zhu S, Liu L, Korzh V, Gong Z, Low BC. RhoA acts downstream of Wnt5 and
567 Wnt11 to regulate convergence and extension movements by involving effectors
568 Rho kinase and Diaphanous: use of zebrafish as an in vivo model for GTPase
569 signaling. Cell Signal. 2006;18(3):359-72.
570 46. Yoshioka K, Nakamori S, Itoh K. Overexpression of small GTP-binding
571 protein RhoA promotes invasion of tumor cells. Cancer Res. 1999;59(8):2004-10.
572 47. Choi SC, Han JK. Xenopus Cdc42 regulates convergent extension
573 movements during gastrulation through Wnt/Ca2+ signaling pathway. Dev Biol.
574 2002;244(2):342-57.
575 48. Reymond N, Im JH, Garg R, Vega FM, Borda d'Agua B, Riou P, et al. Cdc42
576 promotes transendothelial migration of cancer cells through beta1 integrin. J Cell
577 Biol. 2012;199(4):653-68.
578 49. Habas R, Dawid IB, He X. Coactivation of Rac and Rho by Wnt/Frizzled
579 signaling is required for vertebrate gastrulation. . Genes Dev. 2003;17(2):295-
580 309.

581 50. Vega FM, Ridley AJ. Rho GTPases in cancer cell biology. FEBS Lett.
582 2008;582(14):2093-101.
583 51. Marlow F, Topczewski J, Sepich D, Solnica-Krezel L. Zebrafish Rho kinase 2
584 acts downstream of Wnt11 to mediate cell polarity and effective convergence
585 and extension movements. Curr Biol. 2002;12(11):876-84.
586 52. Itoh K, Yoshioka K, Akedo H, Uehata M, Ishizaki T, Narumiya S. An
587 essential part for Rho-associated kinase in the transcellular invasion of tumor
588 cells. Nat Med. 1999;5(2):221-5.
589 53. Kusakabe M, Nishida E. The polarity-inducing kinase Par-1 controls
590 Xenopus gastrulation in cooperation with 14-3-3 and aPKC. EMBO J.
591 2004;23(21):4190-201.
592 54. Shi X, Gangadharan B, Brass LF, Ruf W, Mueller BM. Protease-activated
593 receptors (PAR1 and PAR2) contribute to tumor cell motility and metastasis. Mol
594 Cancer Res. 2004;2(7):395-402.
595 55. Gunaratne A, Thai BL, Di Guglielmo GM. Atypical protein kinase C
596 phosphorylates Par6 and facilitates transforming growth factor beta-induced
597 epithelial-to-mesenchymal transition. Mol Cell Biol. 2013;33(5):874-86.
598 56. Seifert K, Ibrahim H, Stodtmeister T, Winklbauer R, Niessen CM. An
599 adhesion-independent, aPKC-dependent function for cadherins in morphogenetic
600 movements. J Cell Sci. 2009;122(Pt 14):2514-23.
601 57. Yamazaki K, Takamura M, Masugi Y, Mori T, Du W, Hibi T, et al. Adenylate
602 cyclase-associated protein 1 overexpressed in pancreatic cancers is involved in
603 cancer cell motility. Lab Invest. 2009;89(4):425-32.
604 58. Link V, Carvalho L, Castanon I, Stockinger P, Shevchenko A, Heisenberg CP.
605 Identification of regulators of germ layer morphogenesis using proteomics in
606 zebrafish. J Cell Sci. 2006;119(Pt 10):2073-83.
607 59. Khanna C, Wan X, Bose S, Cassaday R, Olomu O, Mendoza A, et al. The
608 membrane-cytoskeleton linker ezrin is necessary for osteosarcoma metastasis.
609 Nat Med. 2004;10(2):182-6.
610 60. Slanchev K, Carney TJ, Stemmler MP, Koschorz B, Amsterdam A, Schwarz
611 H, et al. The epithelial cell adhesion molecule EpCAM is required for epithelial
612 morphogenesis and integrity during zebrafish epiboly and skin development.
613 PLoS Genet. 2009;5(7):e1000563.
614 61. Ni J, Cozzi PJ, Duan W, Shigdar S, Graham PH, John KH, et al. Role of the
615 EpCAM (CD326) in prostate cancer metastasis and progression. Cancer
616 Metastasis Rev. 2012;31(3-4):779-91.
617 62. Skalski M, Alfandari D, Darribere T. A key function for alphav containing
618 integrins in mesodermal cell migration during Pleurodeles waltl gastrulation.
619 Dev Biol. 1998;195(2):158-73.
620 63. Felding-Habermann B. Integrin adhesion receptors in tumor metastasis.
621 Clin Exp Metastasis. 2003;20(3):203-13.
622 64. Marsden M, DeSimone DW. Integrin-ECM Interactions Regulate Cadherin-
623 Dependent Cell Adhesion and Are Required for Convergent Extension in
624 Xenopus. Current Biology. 2003;13(14):1182-91.
625 65. Malik G, Knowles LM, Dhir R, Xu S, Yang S, Ruoslahti E, et al. Plasma
626 fibronectin promotes lung metastasis by contributions to fibrin clots and tumor
627 cell invasion. Cancer Res. 2010;70(11):4327-34.
628 66. Bakkers J, Kramer C, Pothof J, Quaedvlieg NE, Spaink HP, Hammerschmidt
629 M. Has2 is required upstream of Rac1 to govern dorsal migration of lateral cells
630 during zebrafish gastrulation. Development. 2004;131(3):525-37.

631 67. Kim HR, Wheeler MA, Wilson CM, Iida J, Eng D, Simpson MA, et al.
632 Hyaluronan facilitates invasion of colon carcinoma cells in vitro via interaction
633 with CD44. Cancer Res. 2004;64(13):4569-76.
634 68. Coyle RC, Latimer A, Jessen JR. Membrane-type 1 matrix
635 metalloproteinase regulates cell migration during zebrafish gastrulation:
636 evidence for an interaction with non-canonical Wnt signaling. Exp Cell Res.
637 2008;314(10):2150-62.
638 69. Perentes JY, Kirkpatrick ND, Nagano S, Smith EY, Shaver CM, Sgroi D, et al.
639 Cancer cell-associated MT1-MMP promotes blood vessel invasion and distant
640 metastasis in triple-negative mammary tumors. Cancer Res. 2011;71(13):4527-
641 38.
642 70. Cha YI, Kim SH, Sepich D, Buchanan FG, Solnica-Krezel L, DuBois RN.
643 Cyclooxygenase-1-derived PGE2 promotes cell motility via the G-protein-coupled
644 EP4 receptor during vertebrate gastrulation. Genes Dev. 2006;20(1):77-86.
645 71. Kundu N, Fulton AM. Selective cyclooxygenase (COX)-1 or COX-2
646 inhibitors control metastatic disease in a murine model of breast cancer. Cancer
647 Res. 2002;62(8):2343-6.
648 72. Speirs CK, Jernigan KK, Kim SH, Cha YI, Lin F, Sepich DS, et al.
649 Prostaglandin Gbetagamma signaling stimulates gastrulation movements by
650 limiting cell adhesion through Snai1a stabilization. Development.
651 2010;137(8):1327-37.
652 73. Wang D, Dubois RN. Prostaglandins and cancer. Gut. 2006;55(1):115-22.
653 74. Yamashita S, Miyagi C, Fukada T, Kagara N, Che YS, Hirano T. Zinc
654 transporter LIVI controls epithelial-mesenchymal transition in zebrafish gastrula
655 organizer. Nature. 2004;429(6989):298-302.
656 75. Lue HW, Yang X, Wang R, Qian W, Xu RZ, Lyles R, et al. LIV-1 promotes
657 prostate cancer epithelial-to-mesenchymal transition and metastasis through
658 HB-EGF shedding and EGFR-mediated ERK signaling. PLoS One.
659 2011;6(11):e27720.
660 76. Yagi H, Tan W, Dillenburg-Pilla P, Armando S, Amornphimoltham P,
661 Simaan M, et al. A synthetic biology approach reveals a CXCR4-G13-Rho signaling
662 axis driving transendothelial migration of metastatic breast cancer cells. Sci
663 Signal. 2011;4(191):ra60.
664 77. Webster DM, Teo CF, Sun Y, Wloga D, Gay S, Klonowski KD, et al. O-GlcNAc
665 modifications regulate cell survival and epiboly during zebrafish development.
666 BMC Dev Biol. 2009;9:28.
667 78. Lynch TP, Ferrer CM, Jackson SR, Shahriari KS, Vosseller K, Reginato MJ.
668 Critical role of O-Linked beta-N-acetylglucosamine transferase in prostate cancer
669 invasion, angiogenesis, and metastasis. J Biol Chem. 2012;287(14):11070-81.
670 79. Latinkic BV. Xenopus Cyr61 regulates gastrulation movements and
671 modulates Wnt signalling. Development. 2003;130(11):2429-41.
672 80. Lin J, Huo R, Wang L, Zhou Z, Sun Y, Shen B, et al. A novel anti-Cyr61
673 antibody inhibits breast cancer growth and metastasis in vivo. Cancer Immunol
674 Immunother. 2012;61(5):677-87.
675 81. Liu W, Su LT, Khadka DK, Mezzacappa C, Komiya Y, Sato A, et al. TRPM7
676 regulates gastrulation during vertebrate embryogenesis. Dev Biol.
677 2011;350(2):348-57.
678 82. Middelbeek J, Kuipers AJ, Henneman L, Visser D, Eidhof I, van Horssen R,
679 et al. TRPM7 is required for breast tumor cell metastasis. Cancer Res.
680 2012;72(16):4250-61.

681 83. Holloway BA, Gomez de la Torre Canny S, Ye Y, Slusarski DC, Freisinger
682 CM, Dosch R, et al. A novel role for MAPKAPK2 in morphogenesis during
683 zebrafish development. PLoS Genet. 2009;5(3):e1000413.
684 84. Kumar B, Koul S, Petersen J, Khandrika L, Hwa JS, Meacham RB, et al. p38
685 mitogen-activated protein kinase-driven MAPKAPK2 regulates invasion of
686 bladder cancer by modulation of MMP-2 and MMP-9 activity. Cancer Res.
687 2010;70(2):832-41.
688 85. Machingo QJ, Fritz A, Shur BD. A beta1,4-galactosyltransferase is required
689 for convergent extension movements in zebrafish. Dev Biol. 2006;297(2):471-82.
690 86. Zhu X, Jiang J, Shen H, Wang H, Zong H, Li Z, et al. Elevated beta1,4-
691 galactosyltransferase I in highly metastatic human lung cancer cells.
692 Identification of E1AF as important transcription activator. J Biol Chem.
693 2005;280(13):12503-16.
694 87. Hong SK, Tanegashima K, Dawid IB. XIer2 is required for convergent
695 extension movements during Xenopus development. Int J Dev Biol. 2011;55(10-
696 12):917-21.
697 88. Neeb A, Wallbaum S, Novac N, Dukovic-Schulze S, Scholl I, Schreiber C, et
698 al. The immediate early gene Ier2 promotes tumor cell motility and metastasis,
699 and predicts poor survival of colorectal cancer patients. Oncogene.
700 2012;31(33):3796-806.
701 89. Besser J, Leito JT, van der Meer DL, Bagowski CP. Tip-1 induces filopodia
702 growth and is important for gastrulation movements during zebrafish
703 development. Dev Growth Differ. 2007;49(3):205-14.
704 90. Han M, Wang H, Zhang HT, Han Z. The PDZ protein TIP-1 facilitates cell
705 migration and pulmonary metastasis of human invasive breast cancer cells in
706 athymic mice. Biochem Biophys Res Commun. 2012;422(1):139-45.
707 91. Faure S, Cau J, de Santa Barbara P, Bigou S, Ge Q, Delsert C, et al. Xenopus
708 p21-activated kinase 5 regulates blastomeres' adhesive properties during
709 convergent extension movements. Dev Biol. 2005;277(2):472-92.
710 92. Gong W, An Z, Wang Y, Pan X, Fang W, Jiang B, et al. P21-activated kinase 5
711 is overexpressed during colorectal cancer progression and regulates colorectal
712 carcinoma cell adhesion and migration. Int J Cancer. 2009;125(3):548-55.
713 93. Iioka H, Ueno N, Kinoshita N. Essential role of MARCKS in cortical actin
714 dynamics during gastrulation movements. J Cell Biol. 2004;164(2):169-74.
715 94. Rombouts K, Carloni V, Mello T, Omenetti S, Galastri S, Madiai S, et al.
716 Myristoylated Alanine-Rich protein Kinase C Substrate (MARCKS) expression
717 modulates the metastatic phenotype in human and murine colon carcinoma in
718 vitro and in vivo. Cancer Lett. 2013;333(2):244-52.
719
720